Inorganic Chemistry

Article

pubs.acs.org/IC

Synthesis, Characterization, and Spectroscopic Characteristics of Chromium(6+) and -(4+) Silicalite-2 (ZSM-11) Materials

Adrian Lita, Yuchuan Tao, Xisai Ma, Lambertus van de Burgt, and A. E. Stiegman*

Department of Chemistry and Biochemistry, Florida State University, Tallahassee, Florida 32306, United States

Supporting Information

ABSTRACT: The systematic incorporation of Cr ions into a phase-pure silicalite-2 lattice was accomplished through hydrothermal synthesis using 3,5-dimethylpiperidinium as a templating agent. The Cr ions, after calcination to remove the template, were in the 6+ oxidation state, with their incorporation into the lattice verified by the systematic expansion of the unit cell as a function of Cr loading. The structures of these materials as revealed by electronic spectroscopy and X-ray absorption near-edge spectroscopy (XANES) were consistent with the dioxo structure typically exhibited by Cr^{6+} in an amorphous silica matrix. These materials were highly luminescent, with the emission spectra showing an unusually well-resolved vibronic structure characteristic of an emissive site with little inhomogeneous broadening. The site was reduced under flowing CO to Cr^{4+}, as characterized by XANES. The reduction of Cr from 6+ to 4+ resulted in unit-cell volumes that are systematically smaller than those observed with Cr^{6+}, even though the ionic radius of Cr^{4+} is larger. This is attributed to the fact that the Cr^{6+} site is not a simple metal ion but a significantly larger $[CrO_2]^{2+}$ unit, requiring a larger lattice expansion to accommodate it. Through analysis of the XANES preedge and assignment of the ligand-field spectrum of the Cr^{4+} ions, it is possible to establish isomorphic substitution into the silicalite lattice.

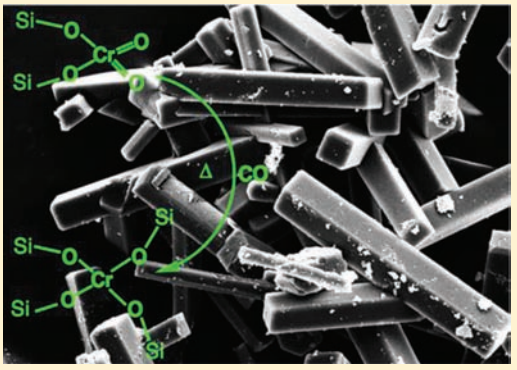

INTRODUCTION

In recent years, there has been considerable interest in molecular-sieve materials containing redox-active transition metals, which act as catalytic sites for performing oxidation reactions.[1] The paradigm for this class of materials is titanium silicalite-1 (TS-1), which contains Ti^{4+} sites distributed in a silicalite-1 (ZSM-5) matrix.[2,3] This system was found to catalyze a number of oxidation reactions using hydrogen peroxide, including the oxidation of phenol to hydroquinone and the epoxidation of vinyl groups.[4] Subsequent to the discovery of TS-1, there have been numerous studies carried out on other transition metals substituted into a number of crystalline and amorphous porous silica materials, including silicalite-1 (ZSM-5) and the related pure silica sieve, silicalite-2 (ZSM-11).[1,5,6] Many of those have been found to exhibit catalytic activity for specific reactions; however, TS-1 remains unique in the number of diverse oxidation processes that it catalyzes both selectively and efficiently.[5−11] One unique aspect of TS-1 that distinguishes it from other metal silicalites is the fact that, because of the net charge 4+ and the small ionic radius of Ti^{4+}, it can isomorphically substitute for tetrahedral Si^{4+} in the silicalite lattice. It is the lability of this coordination environment coupled with the Lewis acidity of the d^0 Ti^{4+} ion that gives rise to much of the observed reactivity.[12] Taking TS-1 as a paradigm, it is likely that other 4+ ions possessing a sufficiently small ionic radius will substitute isostructurally into the silicalite framework. Unfortunately, the majority of other first-row transition metals do not have simple, readily accessible 4+ ions that will be able to isomorphically substitute for Si^{4+}. For example, vanadium has been incorporated into the silicalite-1 lattice.[13,14] After calcination, the oxidation state is 5+, but it always has a terminal oxo group, V═O, with a net charge for the entire group of 3+. This will necessarily balance the charge of only three of the four $Si-O^-$ groups in the silicalite network, leaving a net charge of 1− that is generally assumed to be neutralized by the presence of a proton. Among the possible ions that meet these requirements is Cr^{4+}. This ion has an ionic radius of 0.41 Å, which is close to that of Ti^{4+} (0.56 Å).[15] From a catalytic standpoint, the d^2 electron configuration of this ion will provide ligand stabilization energy, which can affect the coordination of oxidants such as peroxides, thought to be the rate-limiting step in TS-1 oxidations. In principle, this could exert a large effect on the catalytic activity through the effects of the crystal-field activation energy.[16] We report here the synthesis of a silicalite-2 matrix with Cr^{4+} ions substituted into the lattice.

EXPERIMENTAL SECTION

3,5-Dimethyl-*N*,*N*-diethylpiperidinium hydroxide (DDP) were synthesized by published procedures.[17] In a typical preparation of a 1% chromium silicalite, 13.7 mL of a template solution (78.95 mmol of 3,5-dimethyl-*N*,*N*-diethylpiperidinium in 200 mL of an aqueous

Received: August 9, 2011
Published: October 13, 2011

solution) was slowly added with stirring to a mixture comprised of 6 mL of tetraethylorthosilicate and 2 mL of 2-propanol under N_2. To the resultant mixture was added very slowly with vigorously stirring a solution of 0.1094 g of chromium(3+) nitrate nanohydrate in 5.5 mL of nanopure water. The solution was stirred at 70 °C for 3 h. The clear solution obtained was transferred into a Teflon-lined bomb of 250 cm^3 capacity and placed in an oven at 114 °C for 3 days, followed by heating at 175 °C for an additional 4 days. The solid was recovered by centrifugation followed by filtration. The filtrate was washed thoroughly with nanopure water, dried at 120 °C in air for 24 h, and calcined at 500 °C in air for 48 h.

X-ray Diffraction (XRD). Powder XRD patterns were collected on a Siemens D500 diffractometer (40 kV, 30 mA, 2θ 20 min^{-1}) using Cu Kα radiation. The samples were ground to a grain size of 5−10 μm using a mortar and pestle and then mounted on a glass slide using the smear mounting method. Reitveld refinements of the unit-cell parameters were carried out for all diffractions to obtain accurate unit-cell parameters.

Diffuse-Reflectance UV−Visible Spectroscopy. The diffuse-reflectance UV−visible spectra were collected on a Perkin-Elmer-Lambda 900 UV−visible−near-IR spectrophotometer equipped with a 160 mm integrating sphere. The samples were taken from a 500 °C tube furnace into a purged antechamber that also ported to the sample compartment of the N_2-purged spectrometer. The spectra were collected as total reflectance spectra and are displayed in Kubelka−Munk units.

Raman Spectroscopy. Raman spectra of silicalite-2 and chromium(6+) silicalite-2 were obtained using a micro-Raman spectrograph, the JY Horiba LabRam HR800. A Coherent I300C FreD argon-ion laser operating in frequency-doubled mode provided excitation at 244 nm. The use of UV excitation was necessary to avoid fluorescence of chromium(6+) silicalite. It was not possible to avoid fluorescence of Cr^{4+} by either UV or visible (785 nm) excitation; hence, Raman spectra of those materials could not be obtained.

Emission Spectroscopy. Emission spectra of chromium(6+) silicalite-2 were obtained using a 300 mm spectrograph (Acton Research Corp. Spectra Pro 308i, 150 g mm^{-1} grating blazed at 500 nm) and a back-thinned CCD (1340 × 400 pixels, Princeton Instrument LN/CCD-400EB-G1, operated at −90 °C). The sample was mounted in a Supertran-VP continuous-flow (sample in vapor) cryostat (Janis Research Corp.). A Spectra-Physics DCR-3G Nd:YAG laser (10 Hz, 10 ns pulse, 1 J/pulse) operating in the third harmonic provided excitation at 355 nm.

RESULTS AND DISCUSSION

The materials reported here represent an effort to extend the class of isomorphically substituted 4+ metal ions in the silicalite lattice. The particular choice of silicalite-2 (ZSM-11) as the matrix instead of the more common silicalite-1 (ZSM-5) is based on recent studies in our group in the synthesis of silicalite lattices containing the systematic and controllable inclusion of Mn^{2+} and Mn^{3+} ions occupying lattice sites.[18] In these studies, phase-pure silicalite-2 (ZSM-11) was found to be particularly facile in incorporating metal sites into the lattice and, at the same time, provided materials of high crystalline quality, which greatly facilitated characterization. The ZSM-11 and ZSM-5 lattices share similar framework densities and pore sizes; however, the ZSM-5 lattice consists of intersecting straight and curving channels, whereas ZSM-11 topology possesses only straight intersecting channels.[19] In general, these two zeolite structures show similar reactivities.[20] For example, in titanium-substituted silicalite-1 and -2 (TS-1 and TS-2), no significant difference was observed in their catalytic activity toward phenol oxidation with hydrogen peroxide.[21−24]

Cr ions have been incorporated into the silicalite-1 and silicalite-2 lattices.[25−27] Both of these materials were made through the addition of chromium(3+) salts (typically the nitrate) into the silica solid just prior to hydrothermal synthesis. The resulting as-synthesized materials were green in color from their retention of the 3+ oxidation state of the starting chromium salt; however, in all cases, calcination to remove the organic template oxidized the Cr^{3+} site. The final oxidation state of chromium silicalite-1 was found to be 6+, which is the final oxidation state of Cr after high-temperature calcination in most silica matrixes.[28] For chromium silicalite-1, tetrapropylammonium was used as the structure-directing agent (SDA). This produced chromium silicalite-1 of very high crystallographic quality, with chromium incorporation into the lattice established by the unit-cell expansion as measured by XRD. Chromium silicalite-2 was synthesized hydrothermally using tetrabutylammonium (TBA) as the SDA. While these materials catalyzed several notable oxidation processes, TBA is well-known to produce phase-impure silicalite-2, and while a detailed analysis of the crystalline quality was not provided, it is unlikely that these materials were phase-pure.[29,30]

Our approach to creating isomorphically substituted Cr^{4+} ions is to reduce the high-valent Cr sites that form upon calcination of chromium silicalite-1 and -2 down to Cr^{4+} using CO. The initial synthesis of chromium silicalite-2 was carried out hydrothermally at high pH using tetraethylorthosilicate as the silica source and DDP as the SDA. Chromium was introduced as chromium(3+) nitrate nonahydrate into the solid at concentrations ranging from 0.5 to 2.5 mol % Cr to Si. After synthesis, a green powder was recovered from the reaction vessel. This color is consistent with Cr^{3+} ions in silica that were observed in previous syntheses of chromium silicalites.[26,31] Calcination of these materials at 500 °C under air resulted in transformation of the powder from green to orange, with the intensity of the color being dependent upon the amount of chromium.

Powder XRD of calcined (500 °C) 1 mol % chromium silicalite-2 powder gave a well-resolved diffraction pattern, with sharp reflections suggestive of well-formed crystallites (Figure 1a). Analysis of the pattern showed it to be phase-pure ZSM-11, as expected from this SDA, which is confirmed by observation of the diffraction peaks at 2θ = 6.2° and 18.7° associated with the 110 and 330 reflections, respectively, which are allowed for ZSM-11 (MEL) but not ZSM-5 (MFI). In addition, two sharp intense reflections are observed at 2θ = 23.1° for (501) and 23.9° for (303), which are seen in pure-phase ZSM-11 but not in mixed ZSM-11/ZSM-5 materials.[29,30] XRD analysis as a function of added chromium indicates that, up to 2.5 mol %, it remains phase-pure ZSM-11. The unit-cell parameters for each of the chromium silicalite-2 samples were refined in the tetragonal $I4\bar{m}2$ space group of ZSM-11 to obtain an accurate unit-cell volume.

A scanning electron microscopy (SEM) image of the material containing 1 mol % Cr (Figure 2a) shows it to be composed of extremely well-formed crystallites of ∼7 μm in length. Imaging of the crystallites by transmission electron microscopy (TEM) (Figure 2b) reveals well-defined planes with an interplanar spacing of ∼5.4 Å, which corresponds to the (202) crystallographic planes. The material shows a sharp electron diffraction pattern (Figure 2c) that can be readily indexed to the ZSM-11 unit cell. Consistent with what was observed for manganese silicalite-2, the use of DDP to create phase-pure silicalite-2 yields very high-quality, metal-substituted sieves.[18]

The oxidation state of isolated Cr sites in a silica matrix after high-temperature calcination under air typically is 6+.[28] The Cr sites in the silicalite-2 lattice also appear to be in the 6+

dx.doi.org/10.1021/ic2017352 | Inorg. Chem. 2011, 50, 11184−11191

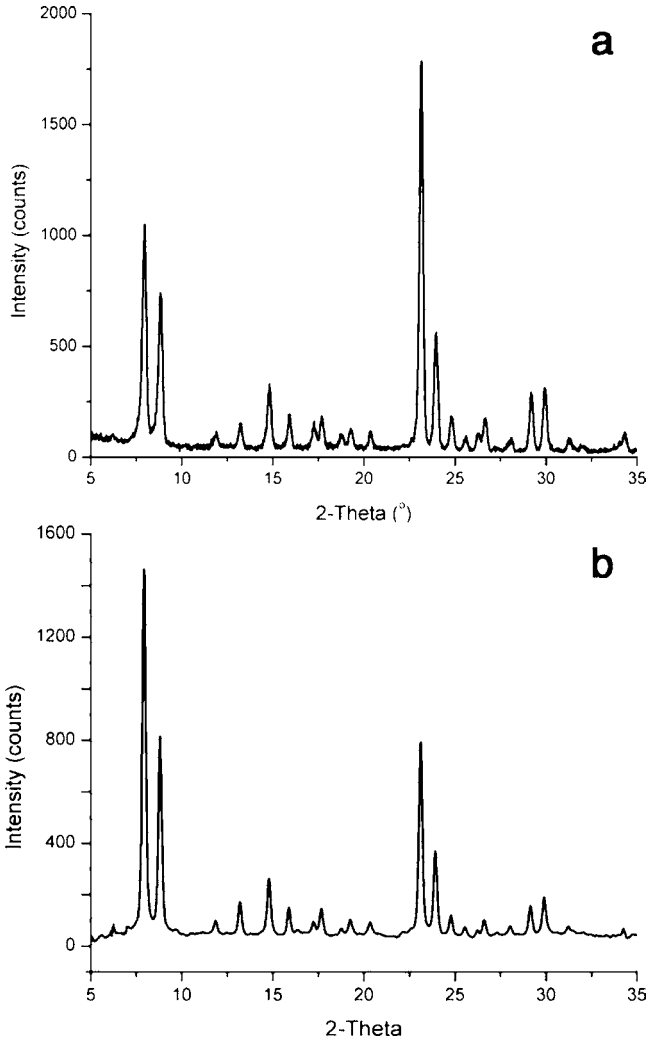

Figure 1. Powder XRD diffractograms of (a) 1% chromium(6+) silicalite-2 and (b) 1% chromium(4+) silicalite-2.

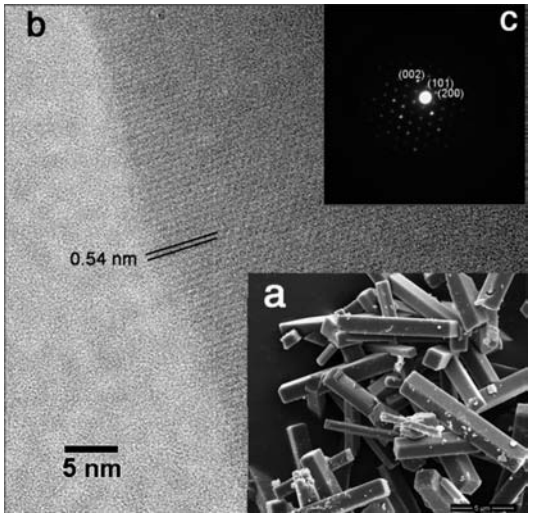

Figure 2. (a) SEM, (b) TEM, and (c) electron diffraction images of 1% chromium(6+) silicalite-2.

oxidation state after calcination. The material is electron paramagnetic resonance silent, which is consistent with diamagnetic Cr^{6+} and also suggests that no residual Cr^{3+} remains in the matrix. Characterization of the materials by X-ray absorption near-edge spectroscopy (XANES), the results of which are shown in Figure 3, reveals a band edge at 6007.2 eV,

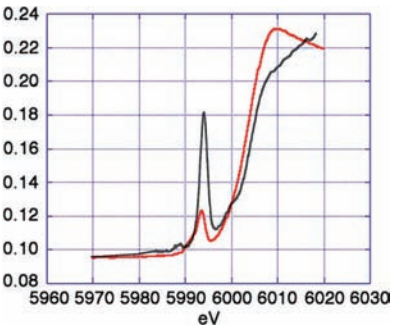

Figure 3. Cr K-edge XANES spectra of (black line) chromium(6+) silicalite-2 and (black line) chromium(4+) silicalite-2.

which is assignable to Cr^{6+}.[32,33] The structure of isolated Cr^{6+} sites in an amorphous silica matrix is well established through vibrational spectroscopy and X-ray absorption fine structure analysis. The sites are four coordinates of nominal C_{2v} symmetry with two terminal oxo groups and two oxygen atoms bridging to silica: $(Si{-}O{-})_2Cr(=O)_2$.[33−36] The energy shift of the edge is governed by its oxidation state and varies almost linearly with the valence of the metal atom if the nature of the atoms in the coordination sphere is not changed (e.g., all are silicate). Thus, it is easy to estimate the oxidation state of chromium by the magnitude of the chemical shift. For the chromium(VI) sample, this is 18 eV from the standard Cr K-edge value of the chromium foil (5989.2 eV). The chromium silica dioxo structure is characterized by a single sharp band occurring in the Raman spectrum at 986 cm^{-1}, which is the highest-energy totally symmetric stretch of the $(Si{-}O{-})_2Cr(=O)_2$ unit that is assigned to a mode that is primarily a stretch of the terminal dioxo group.[33] As can been seen in Figure 4, this

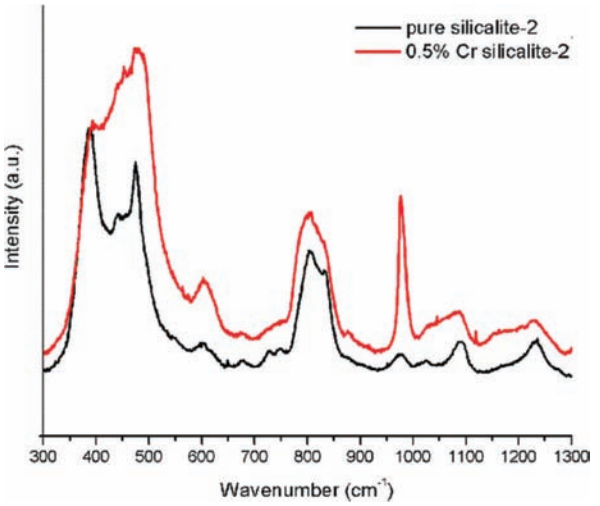

Figure 4. Raman spectra of (black line) silicalite-2 and (red line) 1.0 mol % chromium(6+) silicalite-2 excited at 244 nm.

band is absent in pure silicalite-2 but present in the Raman spectrum of 1% chromium silicalite-2. The presence of this structure-specific spectral feature indicates that, in silicalite-2, the chromium(6+) dioxo structure is retained. The mechanism

dx.doi.org/10.1021/ic2017352 | Inorg. Chem. 2011, 50, 11184–11191

by which the Cr^{3+} ion inserts into the lattice and is oxidized to $(Si{-}O{-})_2Cr(=O)_2$ while yielding materials of good crystallographic quality was not fully elucidated as part of this study. However, in our previous study of manganese($^{2+}$) silicalite-2, we showed that, in the as-synthesized material, the symmetry of the metal ion was very close to octahedral and that the reduction of the symmetry of the metal site to a geometry that is consistent with substitution into a distorted tetrahedral lattice, characteristic of the silicalite, does not occur until calcination takes place.[18] It is reasonable to suggest that chromium insertion into the lattice occurs through a similar process. The green color of the as-synthesized materials is characteristic of octahedral Cr^{3+} in an oxidic environment, suggesting that the ion resides in the silicalite pores, perhaps loosely bound to the framework, with incorporation occurring during high-temperature calcination.[37] The more complex question of when oxidation, which takes Cr^{3+} to Cr^{6+} and places two terminal oxo groups in the coordination sphere of the metal, occurs is not known. It seems unlikely that it occurs after insertion into the lattice because the addition of two terminal oxo groups that would occupy a large volume would tend to be quite disruptive to the lattice. It is more likely that is occurs prior to or concomitant with the calcination process.

A plot of the unit-cell volumes, obtained from the Reitveld refinements of powder XRD, for a series of chromium(6+) silicalite-2 samples of varying chromium concentration is shown in Figure 5. There is a linear increase in the volume as a

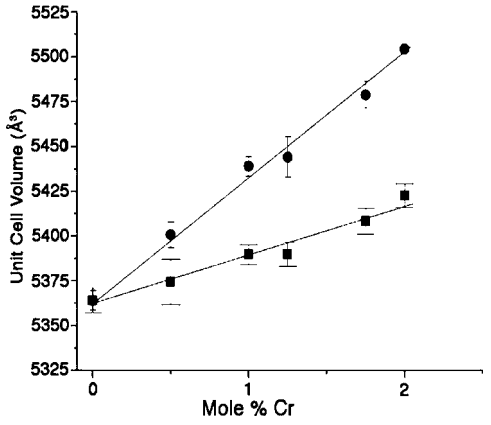

Figure 5. Unit-cell volume as a function of the chromium content for (●) chromium(6+) silicalite-2 and (■) chromium(4+) silicalite-2. Note: the unit-cell volumes for Cr^{6+} and Cr^{4+} at a specific concentration are of the same sample.

function of chromium loading, which is generally taken as indicative of metal ion substitution into the lattice. While it does not quantify the amount of lattice incorporation per amount of added chromium, it does establish that a systematic and proportional incorporation is realized for each loading.

The electronic spectra of the Cr^{6+} sites in amorphous silica, collected as TEM spectra from transparent silica monoliths, have been reported previously.[33] The spectra are characterized by three relatively intense ligand-to-metal charge-transfer (LMCT) bands occurring at [ν (ε)] 22 220 (510), 30 120 (2053), and 41 494 (7470) cm^{-1}. In amorphous silica, the sites show a strong orange luminescence centered around 16 200 cm^{-1}, which, at low temperatures, shows a vibrational progression of approximately 955 cm^{-1}.[33,38] The electronic spectra, collected as diffuse-reflectance spectra, of 2.0 mol % chromium silicalite-2 are shown in Figure 6. The spectrum in Figure 6a shows both of the more intense, high-energy

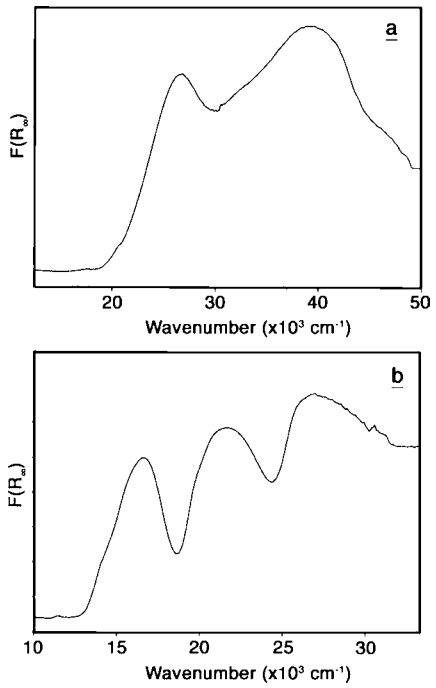

Figure 6. Diffuse-reflectance UV−visible spectra of 2 mol % (a) chromium(6+) and (b) chromium(4+) silicalite-2.

transitions at ~39 560 and 26 700 cm^{-1}; however, the weak low-energy transition is not observed. There are several plausible reasons for this. One is that weak bands are often not observed in diffuse-reflectance spectra because of scattering. The second is that, unlike Cr^{6+} ions dispersed in amorphous silica, the ions in the ZSM-11 lattice are restricted to the seven T sites present in this lattice.[39,40] The specific geometries to which Cr ions are restricted in these sites may well be ones in which orbital overlap between the p orbitals on the bridging oxygen atoms and the metal orbitals is diminished, resulting in decreased intensity for the lowest-energy LMCT transition.

As is observed with Cr^{6+} in amorphous silica, chromium(6+) silicalite-2 shows a strong orange emission, the spectrum of which is shown in Figure 7. This spectrum exhibits an extremely sharp and well-resolved vibronic structure, which is characterized by a high-frequency progression at a frequency of approximately 985 cm^{-1} with an origin at 16 505 cm^{-1}, which we tentatively assign as E_{00} because no bands to higher energy are observed. Upon each mode of the high-frequency progression is built a low-frequency progression at ~227 cm^{-1}. While a more detailed analysis of the spectroscopy will be provided in a future publication, we can reasonably assign the high-frequency mode to the vibration associated with the $(Si{-}O{-})_2Cr(=O)_2$ symmetric stretching mode observed in the Raman spectrum (Figure 4). The 227 cm^{-1} mode is less obvious, and because of its low frequency, it is not directly observed spectroscopically. Fortunately, high-quality calculations by Dines and Inglis predict a relatively intense, totally symmetric low-frequency mode at 214 cm^{-1} that is a normal mode dominated by O−Cr−O bending motion, which is a reasonable assignment for this mode.[41] The observation of such a well-resolved vibronic structure is notable for several reasons. Vibronically resolved emission spectra have been observed for

dx.doi.org/10.1021/ic2017352 | Inorg. Chem. 2011, 50, 11184–11191

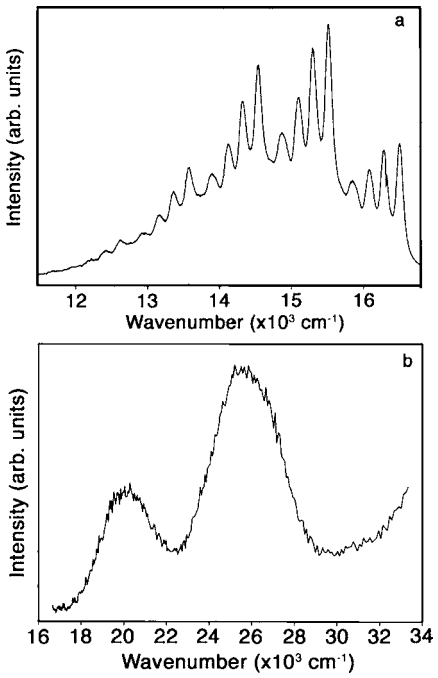

Figure 7. (a) Emission (355 nm ex) and (b) excitation (644 nm monitor) spectra of a 0.5 mol % chromium(6+) silicalite-2 sample collected at 77 K.

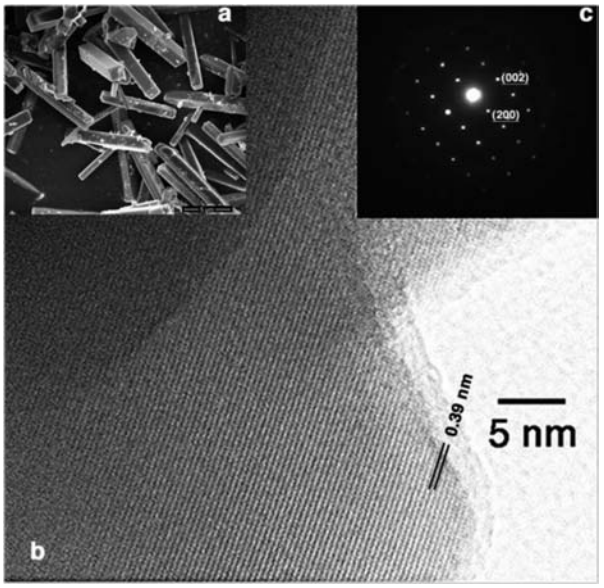

Figure 8. (a) SEM, (b) TEM, and (c) electron diffraction images of a calcined (500 °C under O_2) 1 mol % chromium(4+) silicalite-2 sample.

several d^0 metal ions on silica; however, all of these have shown broad, poorly resolved vibronic progressions, usually in a frequency range between ~960 and 1000 cm^{-1}. The broadness is generally attributed to inhomogeneous broadening arising from the distribution of coordination geometries that the metal site can adopt in the amorphous silica matrix.[38,42,43] The sharp, well-resolved emission lines in the crystalline silicalite-2 matrix are clearly indicative of a well-ordered system with minimal inhomogeneous broadening. Such a well-resolved vibronic structure has been observed in the absorption bands of tetrahedral CrO_4^{2-} doped into Li_3PO_4, where the Cr^{6+} ions reside in a well-defined crystallographic site.[44] Finally, the emission excitation spectrum was collected and is shown in Figure 8. As can be seen, the low-energy transition that was not observed in the UV−visible spectrum is clearly observed in the emission excitation spectrum, where it is at ~20 500 cm^{-1}. This confirms our prior suggestion that the low-energy transition is present but simply too weak to be observed in these materials.

The reduction of silica-supported chromium(6+) oxide by CO has been intensely studied because of its importance in activating these materials for use as the Phillips ethylene polymerization catalyst.[28] Studies by Krauss have shown that CO reduction of silica-supported Cr^{6+} sites passes through a Cr^{4+} intermediate during formation of the Phillips catalyst.[45] The reaction of chromium(6+) silicalite-2 with CO was carried out thermally at 220 °C. This threshold for the reaction was determined qualitatively from the observable color changes in the material as a function of the temperature. The reaction was carried out under flowing CO (1 atm), realizing only slight color changes in the material after 8 h. After 32 h, a much more dramatic color change was observed, suggesting that a more significant amount of the reaction had occurred. The electronic spectrum of 2.00% chromium silicalite-2 after reduction at 240 °C for 32 h is shown in Figure 6b. A definitive assignment of the 4+ oxidation state was established by XANES spectroscopy (Figure 3), which shows the Cr K-edge at 6004.4 eV, which is close to the K-edge of a chromium(4+) reference sample [bis(neopentyl)chromium(4+) on silica], which was measured by us and found to occur at 6004.2 eV.[32]

Because our goal is to create isomorphic substitution of Cr^{4+} in the silicalite lattice, it is important to assess whether this has been accomplished. A reasonable pathway by which the chromium(6+) dioxo species could be transformed into an isomorphically coordinated Cr^{4+} site involves a two-electron reduction by CO with concomitant removal of a terminal oxygen atom to produce CO_2. The four-coordinate, isomorphic geometry is obtained, either subsequently or concertedly, by condensation of the remaining terminal oxygen atom with the neighboring silanols to generate the Cr^{4+} site with elimination of water (reaction 1).

$$(Si-O)_2Cr(=O)_2 + 2SiOH + CO \rightarrow (Si-O)_4Cr + H_2O + CO_2 \quad (1)$$

Analysis by XRD verifies that chromium(4+) silicalite-2 is still phase-pure ZSM-11 of apparently good crystallinity (Figure 1b), even after the high-temperature reduction process. The diffraction peaks are as sharp as those of the Cr^{6+} starting materials, indicating high crystal quality. This is further confirmed by SEM (Figure 8a), which shows the crystals to be very well-formed rods, on the order of 7−15 μm long and 1.68 μm square, which are identical in habit to the materials calcined at 500 °C, with no obvious evidence of degradation. Similarly, TEM (Figure 8b) of the crystallites reveals well-defined planes with an interplanar spacing of ~7.5 Å, which corresponds to the (211) crystallographic planes. The material shows an electron diffraction pattern (Figure 8c) that is indexed to the ZSM-11 unit cell.

Expansion of the unit-cell volume as a function of the chromium content is observed for the Cr^{4+} materials (Figure 5), suggesting that the ions remain in the lattice sites after reduction, although we cannot rule out that some fraction of them may be expelled from the lattice. Retention of the Cr^{4+}

dx.doi.org/10.1021/ic2017352 | Inorg. Chem. 2011, 50, 11184–11191

ions in the T sites of the silicalite lattice is also supported by the intensity and by the slight change in the position of the preedge feature, which is apparent in the XANES (Figure 3) at ~5993.5 eV.[46] The intensity of the preedge will depend strongly on the symmetry of the Cr site and on the oxidation state.[47] In going from Cr^{6+} to Cr^{4+} in a tetrahedral geometry, the preedge intensity drops significantly, by as much as half.[46,47] As such, the decrease in the intensity of about two-thirds that we observe between Cr^{6+} in a fully allowed C_{2v} symmetry and Cr^{4+} in a symmetry that is nominally tetrahedral, but in actuality is distorted from that depending on the exact T site(s) occupied, is consistent.

It is interesting to compare the unit-cell volume changes that occur when Cr^{6+} is reduced to Cr^{4+}. For a given concentration of chromium, the unit-cell volume would be expected to increase when Cr^{6+} is reduced to Cr^{4+} because of the change in the ionic radius from 0.26 to 0.41 Å.[15] This is not observed, and, in fact, Cr^{4+} exhibits unit-cell volumes that are systematically lower than those observed with Cr^{6+}. One possible explanation for this is that Cr ions are being ejected from the lattice during the reduction process, thereby reducing the unit-cell volume. While this may contribute to some extent, the data are far too systematic for a random degradation process to be the dominant factor. The percent decrease in the unit-cell volume in going from 6+ to 4+ per mole of Cr ions is relatively constant, though it does decrease somewhat at the highest loading, where ion loss is more likely. A more plausible explanation lies in the fact that the Cr^{6+} site is not a simple metal ion but the molecular $[CrO_2]^{2+}$ unit, which is significantly larger than indicated by the ionic radius alone. Specifically, the radius of the O^{2-} ions is very large (~1.35 Å), and while they are presumably protruding into the empty channel of the zeolite, the lattice must expand to accommodate this molecular unit.[15] Importantly, because the $[CrO_2]^{2+}$ unit is divalent, it will formally neutralize only two of the Si−O− groups in the lattice, while the remainder of the charge will be neutralized by protons. This will provide a larger coordination sphere around the metal to accommodate the size of the ion. The steric restrictions imposed by the CrO_2 unit may well restrict substitution to a specific lattice site (or a small subset of sites) that can accommodate it. Such site selectivity is difficult to prove; however, the extremely well-resolved vibronic structure observed in the Cr^{6+} emission spectra is certainly consistent with a well-defined coordination geometry imposed by a specific crystallographic site.

Because of their potential application as IR lasing chromophores, the spectroscopy and electronic structure of Cr^{4+} ions in four-coordinate tetrahedral or distorted tetrahedral crystalline environments have been studied extensively and are well understood.[48,49] As such, if the Cr^{4+} ions in the silicalite lattice have a similar coordination environment, as would necessarily arise from isostructural substitution of the Si ions, then the electronic spectra should be consistent with what is observed for other four-coordinate oxidic environments. The electronic spectrum of a sample of 2 mol % chromium(4+) silicalite-2, measured as a diffuse-reflectance spectrum, is shown in Figure 6b. The spectrum is consistent with d^2 ions in a tetrahedral environment, where there are three spin-allowed transitions: an orbitally forbidden $^3A_2 \rightarrow {}^3T_2(F)$ transition, which lies at lower energy, and two fully allowed transitions to $^3T_1$ excited states [$^3A_2 \rightarrow {}^3T_1(F)$ and $^3A_2 \rightarrow {}^3T_1(P)$], which constituent the higher-energy transitions.[37] In small molecules such as $Cr(OBu^t)_4$, which maintain fairly rigorous tetrahedral coordination geometry, these three transitions lie at approximately 9100, 15 200, and 25 000 cm^{-1}, respectively, with the low-energy forbidden band at 9100 cm^{-1} being extremely weak ($\varepsilon \sim 10$).[50] When doped into four-coordinate crystalline environments, like the well-studied olivine structures such as Ca_2GeO_4 and $MgSiO_4$, these same transitions are observed; however, deviations from tetrahedral symmetry intrinsic to the crystallographic sites occupied by the Cr^{4+} ions lead to breaking of the symmetry, which removes the degeneracy of the triply degenerate excited states and produces multiple overlapping transitions in the absorption region. It also relaxes the selection rules so that low-energy transitions to the forbidden $^3T_2$ state are readily observed at ~11 000 cm^{-1}.[44,48,49,51−55] For chromium(4+) silicalite-2, the lowest-energy transitions observed in the spectrum are represented by an extremely weak feature at 11 470 cm^{-1} and three intense, well-resolved peaks at 16 650, 22 290, and 26 900 cm^{-1} (Figure 6b). Assigning the first three bands of chromium(4+) silicalite to the $^3A_2 \rightarrow {}^3T_2$ and $^3T_1$ transitions, from the Tanabe−Sugano diagrams we get the value for the Racah parameter, B, of 547 cm^{-1} and the ligand-field splitting, Δ, of 11 482 cm^{-1}.[37] These values are consistent with ligand-field parameters reported for Cr^{4+} ions in other four-coordinate oxidic environments, although the value of Δ is somewhat larger than is typically reported. In particular, the value Δ reported for $Cr(OBu^t)_4$ was 9430 cm^{-1}, while Cr^{4+} doped into Ca_2GeO_4 and YAG ($Y_3Al_5O_{12}$) has ligand-field splittings that are less than 10 000 cm^{-1}.[50,53−55] However, for the matrixes $MgSiO_4$ and $ZrSiO_4$, Δ values of 10 100 cm^{-1} (B = 560 cm^{-1}) and 10 000 cm^{-1} (B = 500 cm^{-1}), respectively, are observed, reflecting a larger ligand field for the silicate environment, which is consistent with our observations for silicalite.[38,51]

It is reasonable to suggest that structural properties unique to the silicalite lattice give rise to the larger ligand-field splitting and also to the small extinction coefficient of the low-energy $^3A_2 \rightarrow {}^3T_2$ transition. As discussed, deviations from tetrahedral symmetry will have a pronounced effect on the number and intensity of the electronic transitions; these effects have been quantitatively mapped out by Reinen et al. using the angular overlap model.[49] In the silicalite lattice, there are seven T sites that the Cr^{4+} ions can potentially occupy. Coordination of these sites deviates from T_d; however, analysis of the specific geometry of each site from the crystallographic data indicates that distortion from the ideal geometry is small.[30] As can be seen in Table S1 in the Supporting Information, the average value of the bond angles for the sites is 109.5° in all but one site (T-5), with the average deviation of the angles from 109.5° being ~1.5%; similarly, the Si−O bond lengths are ~1.60 Å and vary around the sites by, at most, 1.25%. The small deviation from tetrahedral symmetry does not significantly relax the orbital selection rule that gives rise to the low intensity of the forbidden $^3A_2 \rightarrow {}^3T_2$ transition. The Si^{4+} sites into which Cr^{4+} substitutes have, on average, a shorter metal−oxygen bond distance than is present in most of the olivine structures.[49] It is reasonable to suggest that the short bond distances, coupled with the fact that the silicalite is a rigid network composed entirely of strong Si−O bonds, lead to strongly enforced metal−oxygen interactions that increase the ligand-field splitting. While these structural factors are consistent with the general aspects of the spectra, there is evidence of some degree of splitting of the triply degenerate states. In particular, shoulders are observed at 14 190 and 19 640 cm^{-1} on the side of the two $^3A_2 \rightarrow {}^3T_1$ transitions. Deviations from T_d of the

dx.doi.org/10.1021/ic2017352 | Inorg. Chem. 2011, 50, 11184–11191

various sites, while small, are generally close to D_{2d} symmetry (Table S1 in the Supporting Information), which would break the triple degenerate $^3T_1$ states into A_2 and E states, transitions that may be responsible for the observed shoulders. It is important to note, however, that in these materials different sites, with differing degrees of distortion from T_d, may be occupied, which can complicate the spectral features, thus making detailed assignments difficult. Notably, the spectra also show a broad intense band at higher energy (~26 900 cm^{-1}), which, because of its intensity, is assigned to a CT transition.[50]

In summary, we have shown that Cr ions could be successfully substituted into the framework of a silicalite-2 lattice to generate, initially, after calcination, a chromium(6+) silicalite-2 molecular sieve. These materials, while serving as a synthetic precursor for making chromium(4+) silicalte-2, proved to have unusual spectroscopic properties; in particular, they exhibited an extremely well-resolved vibronic structure. Reduction of Cr^{6+} to isovalent Cr^{4+} sites was accomplished through high-temperature reduction with CO. The resulting materials retained their high crystallographic quality, and on the basis of analysis of the XANES preedge feature and the electronic spectrum of the chromium(IV) ligand-field bands, it appears that the Cr^{4+} sites are four-coordinate and isostructural with the Si ions in the lattice. This establishes that chromium(4+) silicalite-2 is a material that is similar to the titanium silicalite class of oxidation catalysts in terms of the valency and coordination environment of the active site, although different in their ligand-field properties, and, hence, is a viable candidate for catalytic activity.

■ ASSOCIATED CONTENT

Ⓢ Supporting Information

Table S1 of T-site geometries for silicalite-2 and their deviation from tetrahedral. This material is available free of charge via the Internet at http://pubs.acs.org.

■ AUTHOR INFORMATION

Corresponding Author

*E-mail: stiegman@chem.fsu.edu.

■ ACKNOWLEDGMENTS

The work was carried out under the auspices of the National Science Foundation (Grant NSF-CHE 0911080).

■ REFERENCES

(1) Arends, I. W. C. E.; Sheldon, R. A.; Wallau, M.; Schuchardt, U. *Angew. Chem., Int. Ed. Engl.* **1997**, *36*, 1145.
(2) Notari, B. *Catal. Today* **1993**, *18*, 163.
(3) Notari, B. *Adv. Catal.* **1996**, *41*, 253.
(4) Smith, G. V.; Notheisz, F. *Heterogeneous catalysis in organic chemistry*; Academic Press: San Diego, 1998 .
(5) Luna, F. J.; Schuchardt, U. *Quim. Nova* **2001**, *24*, 885.
(6) Tuel, A. In *Mesoporous Molecular Sieves*; Bonneviot, L., Beland, F., Danumah, C., Giasson, S., Kaliaguine, S., Eds.; Elsevier Science Publishing BV: Amsterdam, The Netherlands, 1998; Vol. *117*, p 159.
(7) Choi, J. S.; Yoon, S. S.; Jang, S. H.; Ahn, W. S. *Catal. Today* **2006**, *111*, 280.
(8) Hartmann, M.; Ernst, S. *Angew. Chem., Int. Ed.* **2000**, *39*, 888.
(9) Ribera, A.; Arends, I.; de Vries, S.; Perez-Ramirez, J.; Sheldon, R. A. *J. Catal.* **2000**, *195*, 287.
(10) Samanta, S.; Mal, N. K.; Bhaumik, A. *J. Mol. Catal. A: Chem.* **2005**, *236*, 7.
(11) Wang, F.; Yang, G. Y.; Zhang, W.; Wu, W. H.; Xu, J. *Adv. Synth. Catal.* **2004**, *346*, 633.
(12) Corma, A.; Garcia, H. *Chem. Rev.* **2002**, *102*, 3837.
(13) Reddy, J. S.; Sayari, A. *Catal. Lett.* **1994**, *28*, 263.
(14) Tatsumi, T.; Hirasawa, Y.; Tsuchiya, J. *Heterogeneous Hydrocarbon Oxidation* **1996**, *638*, 374.
(15) Shannon, R. D. *Acta Crystallogr., Sect. A* **1976**, *32*, 751.
(16) Basolo, F.; Pearson, R. G. *Mechansims of Inorganic Reactions*; John Wiley & Sons: New York, 1967.
(17) Nakagawa, Y. U.S. Patent 5,645,812, 1997.
(18) Lita, A.; Ma, X. S.; Meulenberg, R. W.; van Buuren, T.; Stiegman, A. E. *Inorg. Chem.* **2008**, *47*, 7302.
(19) Kustova, M. Y.; Kustov, A.; Christiansen, S. E.; Leth, K. T.; Rasmussen, S. B.; Christensen, C. H. *Catal. Commun.* **2006**, *7*, 705.
(20) Zhang, L.; Liu, H.; Li, X.; Xie, S.; Wang, Y.; Xin, W.; Liu, S.; Xu, L. *Fuel Proc. Technol.* **2010**, *91*, 449.
(21) Tuel, A.; Bentaarit, Y. *Appl. Catal., A* **1993**, *102*, 69.
(22) Reddy, J. S.; Kumar, R. *Zeolites* **1992**, *12*, 95.
(23) Reddy, J. S.; Sivasanker, S. *Indian J. Technol.* **1992**, *30*, 64.
(24) Reddy, J. S.; Sivasanker, S.; Ratnasamy, P. *J. Mol. Catal.* **1992**, *71*, 373.
(25) Jayachandran, B.; Sasidharan, M.; Sudalai, A.; Ravindranathan, T. *J. Chem. Soc., Chem. Commun.* **1995**, 1523.
(26) Joseph, R.; Sasidharan, M.; Kumar, R.; Sudalai, A.; Ravindranathan, T. *J. Chem. Soc., Chem. Commun.* **1995**, 1341.
(27) Vanderpull, N.; Jansen, W. J. C.; Vanbekkum, H. In *Zeolites and Related Microporous Materials: State of the Art*; Weitkamp, J., Karge, H. G., Pfeifer, H., Holderich, W., Eds.; Elsevier Science Publishing BV: Amsterdam, The Netherlands, 1994; Vol. *84*, p 211.
(28) Weckhuysen, B. M.; Wachs, I. E.; Schoonheydt, R. A. *Chem. Rev.* **1996**, *96*, 3327.
(29) Piccione, P. M.; Davis, M. E. *Microporous Mesoporous Mater.* **2001**, *49*, 163.
(30) Terasaki, O.; Ohsuna, T.; Sakuma, H.; Watanabe, D.; Nakagawa, Y.; Medrud, R. C. *Chem. Mater.* **1996**, *8*, 463.
(31) Mambrim, J. S. T.; Pastore, H. O.; Davanzo, C. U.; Vichi, E. J. S.; Nakamura, O.; Vargas, H. *Chem. Mater.* **1993**, *5*, 166.
(32) Arcon, I.; Mirtic, B.; Kodre, A. *J. Am. Ceram. Soc.* **1998**, *81*, 222.
(33) Moisii, C.; Deguns, E. W.; Lita, A.; Callahan, S. D.; van de Burgt, L. J.; Magana, D.; Stiegman, A. E. *Chem. Mater.* **2006**, *18*, 3965.
(34) Weckhuysen, B. M.; Schoonheydt, R. A.; Jehng, J. M.; Wachs, I. E.; Cho, S. J.; Ryoo, R.; Kijlstra, S.; Poels, E. *J. Chem. Soc., Faraday Trans.* **1995**, *91*, 3245.
(35) Weckhuysen, B. M.; Spooren, H. J.; Schoonheydt, R. A. *Zeolites* **1994**, *14*, 450.
(36) Weckhuysen, B. M.; Wachs, I. E. *J. Phys. Chem.* **1996**, *100*, 14437.
(37) Lever, A. B. P. *Inorganic Electronic Spectroscopy*, 2nd ed.; Elsevier: Amsterdam, The Netherlands, 1984.
(38) Hazenkamp, M. F.; Blasse, G. *J. Phys. Chem.* **1992**, *96*, 3442.
(39) Bibby, D. M.; Milestone, N. B.; Aldridge, L. P. *Nature* **1979**, *280*, 664.
(40) Kokotailo, G. T.; Chu, P.; Lawton, S. L.; Meier, W. M. *Nature* **1978**, *275*, 119.
(41) Dines, T. J.; Inglis, S. *Phys. Chem. Chem. Phys.* **2003**, *5*, 1320.
(42) Soult, A. S.; Carter, D. F.; Schreiber, H. D.; van de Burgt, L. J.; Stiegman, A. E. *J. Phys. Chem. B* **2002**, *106*, 9266.
(43) Tran, K.; Hanninglee, M. A.; Biswas, A.; Stiegman, A. E.; Scott, G. W. *J. Am. Chem. Soc.* **1995**, *117*, 2618.
(44) Atanasov, M.; Brunold, T. C.; Gudel, H. U.; Daul, C. *Inorg. Chem.* **1998**, *37*, 4589.
(45) Kohler, S. D.; Ekerdt, J. G. *J. Phys. Chem.* **1994**, *98*, 4336.
(46) Pantelouris, A.; Modrow, H.; Pantelouris, M.; Hormes, J.; Reinen, D. *Chem. Phys.* **2004**, *300*, 13.
(47) Yamamoto, T. *X-ray Spectrom.* **2008**, *37*, 572.
(48) Reinen, D.; Kesper, U.; Atanasov, M.; Roos, J. *Inorg. Chem.* **1995**, *34*, 184.
(49) Reinen, D.; Rauw, W.; Kesper, U.; Atanasov, M.; Gudel, H. U.; Hazenkamp, M.; Oetliker, U. *J. Alloys Compd.* **1997**, *246*, 193.
(50) Alyea, E. C.; Basi, J. S.; Bradley, D. C.; Chisholm, M. H. *J. Chem. Soc. A* **1971**, 772.

(51) Belletti, A.; Borromei, R.; Oleari, L. *Inorg. Chim. Acta* **1995**, *235*, 349.
(52) Atanasov, M. *Chem. Phys. Lett.* **1995**, *234*, 313.
(53) Hazenkamp, M. F.; Gudel, H. U.; Atanasov, M.; Kesper, U.; Reinen, D. *Phys. Rev. B* **1996**, *53*, 2367.
(54) Hazenkamp, M. F.; Oetliker, U.; Gudel, H. U.; Kesper, U.; Reinen, D. *Chem. Phys. Lett.* **1995**, *233*, 466.
(55) Eilers, H.; Hommerich, U.; Jacobsen, S. M.; Yen, W. M.; Hoffman, K. R.; Jia, W. *Phys. Rev. B* **1994**, *49*, 15505.